

Study on Micro Structural Properties of Sodium in Na₂O - Doped SiO₂ Melt using Molecular Dynamics Simulation

Abstract. We built molecular dynamics (MD) simulations to investigate micro-structural properties of sodium in Na₂O-doped SiO₂ melt through Voronoi polyhedron. The result shows that many bridging oxygen (BO) polyhedrons and all Si-polyhedrons do not contain Na atom. Most non-bridging oxygen (NBO) polyhedrons contain 2, 1 or not Na atoms, where BO, NBF is the O bonded with 2 and 1 or not Si, respectively. Average volume per polyhedron decreases in order: NBF_x-polyhedron → BO_x-polyhedron → Six-polyhedron. Sodium atoms are found in NBF_x-polyhedrons and frequently move through them leading to very fast diffusivity of Na in comparison with Si and O. The simulation shows that the number of neighbors around the NBF_x-polyhedron is larger than that around the BO_x-polyhedron.

Keywords: Na₂O-doped SiO₂, sodium, Voronoi polyhedron, micro-structure, subnets.

1. Introduction

The micro-structure of silica (SiO₂) is an archetypal network-forming system containing SiO₄ tetrahedra. The addition of doped Na atoms generates non-bridging oxygen (NBO) in SiO₄. Consequently, the Na₂O-doped SiO₂ gives various anomalous properties which are essential for industrial applications, ceramics, and understanding the fundamentals of minerals [1-5]. The Na₂O-doped SiO₂ melt has been intensively investigated by experimental techniques including photoelectron spectroscopy, X-ray diffraction, in situ Raman spectroscopy and elastic neutron scattering, and various simulation techniques [6-11]. The addition of doped Na ions to pure SiO₂ melt leads to a decoupling of alkali diffusion and diffusive transport in the Si-O network [10-17]. Davidenko et al. in ref. [7] suggested that the distribution where the increasing alkali oxide content causes the homogeneous increasing disruption of Si-O network of pure SiO₂ is in conflict with highly nonlinear dependence of viscosity on alkali concentration. In accordance with studies [18-21], the pre-peak at 0.9 Å⁻¹ in the micro-structure factor measured experimentally for alkali silicates is evidence for the diffusion pathway.

Various experimental results found that the micro-structure of these silicates is found to comprise micro-regions with high sodium concentration. The two micro structural samples, the modified random network and the compensated continuous random network predict some clustering of alkali atoms in the silicate's microstructure [22-24].

However, the spatial distribution of Na in the Na₂O-doped SiO₂ melt remains not fully clarified yet. Therefore, in present study, we focus on Na₂O-xSiO₂ melt (x = 1, 2, 3, 4) at pressure of 0.1 MPa and temperatures of 1573 K. Based on the features of pair radial distribution function (PRDF), topographies of the Voronoi A_x- polyhedrons, and subnets Si-O in system.

2. Computational method

We conduct the MD simulation for NS_x, i.e. Na₂O-SiO₂ (NS1), Na₂O-2SiO₂ (NS2), Na₂O-3SiO₂ (NS3) and Na₂O-4SiO₂ melt at pressure of 0.1 MPa and temperature of 1573 K. The total number of particles in each system is approximately equal to 10,000. The interaction potentials used includes two- and three-body terms, which reproduce well the micro structural and transport properties of sodium silicates. The complete description of these potentials can be found elsewhere [4,25]. In order to collect the micro-structure and dynamics data we additionally run the simulation for 150 ps to produce 76 configurations separated by 2 ps. The structure is analyzed by PRDF and by the one determined separately for BO and NBF. Here BO, NBO and FO are the oxygen which is bounded respectively with two, one or not Si; both NBO and FO are denoted to NBF.

Si-BO subnet, Si- and O-centered Voronoi polyhedrons have been calculated for every system. It turns out that the simulation box is fully filled by those polyhedrons. Each Na is placed inside one among them. Several typical polyhedrons are shown in Figure 1. The following, A-centered polyhedron is called an A_x-polyhedron, where A is the Si, O, BO or NBF; *x* is the number of Na placed in A-centered polyhedron. We call that all Six-polyhedrons and a part of O_x-polyhedrons are A₀-polyhedron type. Moreover, Na often moves between O_x-polyhedrons leading to very fast sodium diffusivity. Fig.1 illustrates the system comprising a large Si-O subnet. The Si-O subnet is defined as a subset of Si and BO connected by Si-O bonds, where BO is bonded with two Si, while Si is bonded with four O forming the SiO₄ unit.

3. Results and discussions

To check the value of the simulation samples, we compared the position of the first peak of PRDF with experimental data. Table 1 lists the interatomic distances obtained from simulation, and experimental data [29]. Although r_{SiNa} and r_{NaNa} show some discrepancies, the built models overall are consistent with the experiments. In particular, they reproduce the experimental data for r_{SiSi} , r_{SiO} , r_{OO} , and r_{NaO} .

Samples	r_{SiSi}	r_{SiO}	r_{OO}	r_{SiNa}	r_{ONa}	r_{NaNa}
NS1	3.10	1.60	2.60	3.00	2.20	3.25
NS2	3.10	1.60	2.60	3.30	2.25	3.50
NS3	3.10	1.55	2.60	3.35	2.25	3.65
NS4	3.10	1.60	2.60	3.40	2.25	3.60
Exp. [26]	3.05	1.62	2.62	3.50	2.29	2.6-3.05

Figure 2 shows the PRDF determined for BO-Na, NBF-Na and O-Na pairs. A clear peak is seen for the NBF-Na pair, with a significant increase in height from NS1 to NS4. The location of this peak is slightly different. For the BO-Na pair, the height of the first peak is much lower than for the NBF-Na pair. This result indicates that Na atoms are mostly located around NBF and rarely near BO. Furthermore, the local sodium density in BO_x and NBF_x polyhedra changes strongly with SiO concentration. Unlike the NBF-Na pair, the first peak of the Si-Na pair is located at 3.0-3.6 Å, which is significantly larger than that of the NBF-Na pair. This means that Na is not in the Six-polyhedrons. These marks are consistent with the reports in refs. [1-6].

Figure 3 shows snapshots of the distribution of coordination units SiO_x and NaO_y in a model of $\text{Na}_2\text{O}-3\text{SiO}_2$ melt at a pressure of 0.1 GPa (here we only draw a part with size $6 \times 20 \times 20 \text{ \AA}^3$). Figure 3 indicates that the micro-structure of $\text{Na}_2\text{O}-3\text{SiO}_2$ melt comprises the coordination units SiO_4 , and some NaO_4 , NaO_5 . From Figure 3, it can be seen that the distribution of coordination units SiO_4 is not uniform. Still, it tends to form clusters of SiO_4 , and the coordination units SiO_4 tend to connect via a common oxygen atom to form subnet Si-O. Similarly, the coordination NaO_4 tends to connect to create a cluster of NaO_4 , and the $\text{Na}_2\text{O}-3\text{SiO}_2$ melt only contains some coordination NaO_5 . Therefore, the micro-structure of $\text{Na}_2\text{O}-3\text{SiO}_2$ melt is built up from the intermixture of the clusters SiO_4 , NaO_4 , NaO_5 , and free Na.

Table 2 shows the average volume per polyhedron in descending order: NBFx-polyhedron \rightarrow BOx-polyhedron \rightarrow Six-polyhedron, and it slightly varies with SiO_2 content. We note that $\langle x_{\text{NBFx}} \rangle$ is significantly larger than $\langle x_{\text{BOx}} \rangle$. Moreover, $\langle x_{\text{BOx}} \rangle$ changes powerfully with SiO_2 content. This result shows that the spatial distribution of sodium is strongly heterogeneous. In particular, the most important Na is located in NBFx polyhedra with a total volume of 27.11–67.10% of the simulation box. In the system with lower SiO_2 content, more Na diffused into the Box-polyhedron.

Table 2. Characteristics of Ax-polyhedrons. Here $\langle v_{\text{Six}} \rangle$, $\langle v_{\text{BOx}} \rangle$ and $\langle v_{\text{NBFx}} \rangle$ is the average volume per Six-, BOx- and NBFx-polyhedron, respectively; V_{Six} , V_{BOx} , V_{NBFx} and V_{SB} is the volume occupied by Six-, BOx-, NBFx-polyhedrons and volume of simulation box, respectively; m_{NBF} , N_{Na} is the number of Na in NBFx-polyhedrons and total number of Na, respectively.

System	$\langle v_{\text{Six}} \rangle, \text{ \AA}^3$	$\langle v_{\text{BOx}} \rangle, \text{ \AA}^3$	$\langle v_{\text{NBFx}} \rangle, \text{ \AA}^3$	$V_{\text{Six}}/V_{\text{SB}}$	$V_{\text{BOx}}/V_{\text{SB}}$	$V_{\text{NBFx}}/V_{\text{SB}}$	$m_{\text{NBF}}/N_{\text{Na}}$
NS1	8.13	20.12	30.41	0.0920	0.2370	0.6710	0.8682
NS2	7.96	20.25	31.45	0.1140	0.4369	0.4491	0.8081
NS3	7.94	20.37	31.96	0.1260	0.5379	0.3361	0.7909
NS4	7.94	20.44	32.45	0.1324	0.5965	0.2711	0.7798

Different Six-polyhedrons, Ox-polyhedrons either are polyhedrons with $x_{\text{Ox}} = 0$ or $x_{\text{Ox}} > 0$. As shown in Figure 4, the number of BO0-polyhedrons increases from 78.1 to 95.8% with increasing SiO_2 content. Figure 4 shows that most Box-polyhedrons are BO0 and BO1 polyhedrons, while the most important NBFx- polyhedrons are either NBF0, NBF1, and NBF2 polyhedrons. In addition, the Na atoms are concentrated in the NBFx-polyhedrons instead of being uniformly distributed in the Ox- polyhedrons. The obtained result makes it possible to propose a simple diffusion model. Consequently, Na moves from BOx and NBFx- polyhedron sites. Each slot is empty or occupied by one Na in BOx- polyhedron, an NBFx polyhedron has one and two points respectively. There are also torus polyhedrons with more than 2 sites, but their concentration is very low. Na transfer between Ox- polyhedrons results in very fast diffusion of Na compared to Si and O [10,20].

The sodium distribution in polyhedrons shown in Figure 5, it can be wide and asymmetrical. A pronounced peak is seen. This result confirms the fact that Na atoms are concentrated in NBF-polyhedrons instead of uniformly distributed through O-polyhedrons.

In summary, Na atoms are concentrated in NBF-polyhedrons instead of uniformly spreading through O-polyhedrons. The frequent displacing of Na between polyhedrons mainly

contributes to the sodium's diffusion. The system consists of the NBO-FO, interfacial and Si-BO regions. The rate of $Ax \rightarrow Ax'$ happening in those regions reduces in the order: NBO-FO region \rightarrow interface region \rightarrow Si-BO region. Therefore, our results can propose that Na atoms diffuse by hopping alone and collective movement, but the major amount of Na moves collectively across O-polyhedrons located nearby. For melt with high SiO₂ content the NBO-FO region can represent the preferential sodium's diffusion pathway.

4. Conclusion

MD simulation is carried out for NS_x melt at temperature of 1573 K and pressure of 0.1 GPa. Micro-structural properties are investigated through Voronoi polyhedron. The result shows a pronounced peak for the NBF-Na pair of which the height varies with SiO₂ content. The position of the first peak for Si-Na peak is located at a distance significantly larger than that for the NBF-Na pair. The simulation demonstrates that Na atoms mostly present in the vicinity of NBF and rarely around BO. Simulation reveals that Na atoms are not placed in Six-polyhedrons and in about 32.9 to 72.89 % of total BO_x-polyhedrons. Most NBF_x-polyhedrons contain 2, 1 or not Na. The average volume per polyhedron decreases dramatically in the order: NBF_x-polyhedron \rightarrow BO_x-polyhedron \rightarrow Six-polyhedron. Although the average volume per polyhedron weakly depends on SiO₂ content, the volume occupied by all NBF_x-polyhedrons varies strongly with SiO₂ content. We also discovered that Na atoms are not only located in NBF_x-polyhedrons, but they also move frequently through them. Therefore, we suggest that melt with high SiO₂ content the NBO regions and FO regions can represent the preferential sodium's diffusion pathway.

References

1. Zhong, Cong, et al. "Experimental characterizations and molecular dynamics simulations of the structures of lead aluminosilicate glasses." *Journal of Non-Crystalline Solids* 576 (2022): 121252.
2. Vargheese, K. Deenamma, Adama Tandia, and John C. Mauro. "Molecular dynamics simulations of ion-exchanged glass." *Journal of non-crystalline solids* 403 (2014): 107-112.
3. Yen, N. V., et al. "Spatial distribution of cations through Voronoi polyhedrons and their exchange between polyhedrons in sodium silicate liquids." *Journal of Non-Crystalline Solids* 566 (2021): 120898.
4. Saito, Yoshihiro, Takumi Yonemura, Atsunobu Masuno, Hiroyuki Inoue, Koji Ohara, and Shinji Kohara. "Structural change of Na₂O-doped SiO₂ glasses by melting." *Journal of the Ceramic Society of Japan* 124, no. 6 (2016): 717-720.
- [5] Tuheen, Manzila Islam, Lu Deng, and Jincheng Du. "A comparative study of the effectiveness of empirical potentials for molecular dynamics simulations of borosilicate glasses." *Journal of Non-Crystalline Solids* 553 (2021): 120413.
- [6] Bertani, Marco, et al. "Accurate and Transferable Machine Learning Potential for Molecular Dynamics Simulation of Sodium Silicate Glasses." *Journal of Chemical Theory and Computation* 20.3 (2024): 1358-1370..

- [7] Davidenko, A. O., V. E. Sokol'skii, A. S. Roik, and I. A. Goncharov. "Structural study of sodium silicate glasses and melts." *Inorganic Materials* 50, no. 12 (2014): 1289-1296.
- [8] Zhao, Qing, Michael Guerette, Garth Scannell, and Liping Huang. "In-situ high temperature Raman and Brillouin light scattering studies of sodium silicate glasses." *Journal of non-crystalline solids* 358, no. 24 (2012): 3418-3426.
- [9] Hung, P. K., et al. "Analysis for characterizing the structure and dynamics in sodium disilicate liquid." *Journal of Non-Crystalline Solids* 452 (2016): 14-22.
- [10] Jabraoui, H., E. M. Achhal, A. Hasnaoui, J-L. Garden, Y. Vaills, and S. Ouaskit. "Molecular dynamics simulation of thermodynamic and structural properties of silicate glass: Effect of the alkali oxide modifiers." *Journal of Non-Crystalline Solids* 448 (2016): 16-26.
- [11] Mountjoy, Gavin, Bushra M. Al-Hasni, and Christopher Storey. "Structural organisation in oxide glasses from molecular dynamics modelling." *Journal of non-crystalline solids* 357, no. 14 (2011): 2522-2529.
- [12] Jabraoui, Hicham, Yann Vaills, Abdellatif Hasnaoui, Michael Badawi, and Said Ouaskit. "Effect of sodium oxide modifier on structural and elastic properties of silicate glass." *The Journal of Physical Chemistry B* 120, no. 51 (2016): 13193-13205.
- [13] Voigtmann, Th, and Juergen Horbach. "Slow dynamics in ion-conducting sodium silicate melts: Simulation and mode-coupling theory." *EPL (Europhysics Letters)* 74, no. 3 (2006): 459.
- [14] Thao, N. T., et al. "Study of sodium diffusion in silicate glasses. Molecular dynamics simulation." *Modelling and Simulation in Materials Science and Engineering* 31.8 (2023): 085012.
- [15] Gupta, Y. P., and T. B. King. "Self-diffusion of sodium in sodium silicate liquids." *Transactions of the Metallurgical Society of AIME* 239, no. 11 (1967): 1701.
- [16] Braedt, M., and G. H. Frischat. "Sodium self diffusion in glasses and melts of the system $\text{Na}_2\text{O-Rb}_2\text{O-SiO}_2$." *Physics and chemistry of glasses* 29, no. 5 (1988): 214-218.
- [17] Knoche, Ruth, Donald B. Dingwell, F. A. Seifert, and Sharon L. Webb. "Non-linear properties of supercooled liquids in the system $\text{Na}_2\text{O-SiO}_2$." *Chemical geology* 116, no. 1-2 (1994): 1-16.
- [18] Meyer, A., J. Horbach, W. Kob, Florian Kargl, and H. Schober. "Channel formation and intermediate range order in sodium silicate melts and glasses." *Physical review letters* 93, no. 2 (2004): 027801.
- [19] Kargl, F., H. Weis, T. Unruh, and A. Meyer. "Self diffusion in liquid aluminium." In *Journal of Physics: Conference Series*, vol. 340, no. 1, p. 012077. IOP Publishing, 2012.
- [20] Jund, Philippe, Walter Kob, and Rémi Jullien. "Channel diffusion of sodium in a silicate glass." *Physical Review B* 64, no. 13 (2001): 134303.
- [21] Van, To Ba, P. K. Hung, L. T. Vinh, N. T. T. Ha, L. T. San, and Fumiya Noritake. "Network cavity, spatial distribution of sodium and dynamics in sodium silicate melts." *Journal of Materials Science* 55, no. 7 (2020): 2870-2880.
- [22] Konstantinou, Konstantinos, Dorothy M. Duffy, and Alexander L. Shluger. "Structure and luminescence of intrinsic localized states in sodium silicate glasses." *Physical review B* 94, no. 17 (2016): 174202.

- [23] Greaves, G. N. "Structure and ionic transport in disordered silicates." *Mineralogical Magazine* 64, no. 3 (2000): 441-446.
- [24] Greaves, G. N., and Sabyasachi Sen. "Inorganic glasses, glass-forming liquids and amorphizing solids." *Advances in physics* 56, no. 1 (2007): 1-166.
- [25] Noritake, Fumiya. "Structural transformations in sodium silicate liquids under pressure: New static and dynamic structure analyses." *Journal of Non-Crystalline Solids* 473 (2017): 102-107.
- [26] Fábrián, M., P. Jóvári, E. Sváb, Gy Mészáros, Th Proffen, and E. Veress. Network structure of 0.7SiO₂-0.3Na₂O glass from neutron and x-ray diffraction and RMC modelling. *Journal of Physics: Condensed Matter* 19 (2007) 33, 335209.

UNDER PEER REVIEW

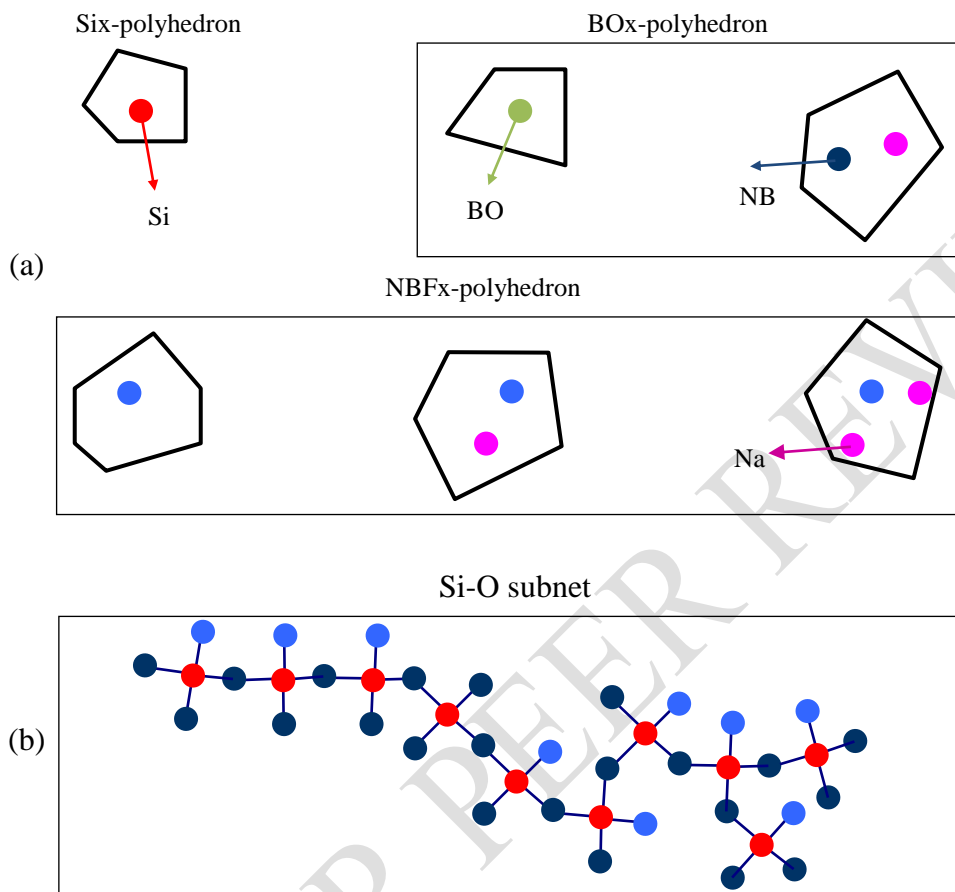


Figure 1. Schematic illustration of A_x -polyhedrons (a) and Si-O subnet (b). Here A is Si, BO or NBF; $x = 0, 1, 2, 3$ and 4. A_x -polyhedron can contain Na atoms.

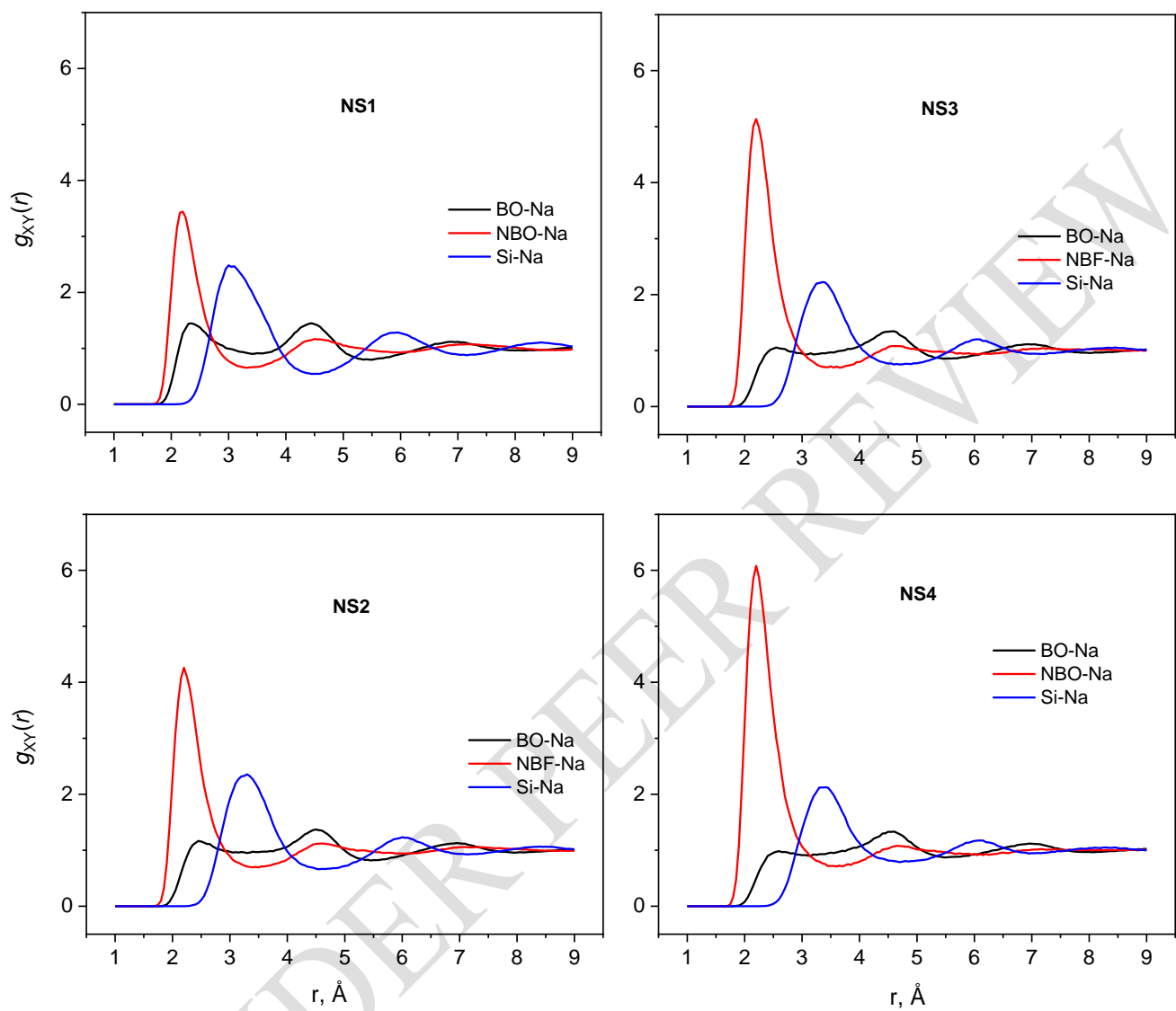


Figure 2. PRDF for NBF-Na, BO-Na, and Si-Na pairs of NSx at temperature of 1573 K and pressure of 0.1 MPa.

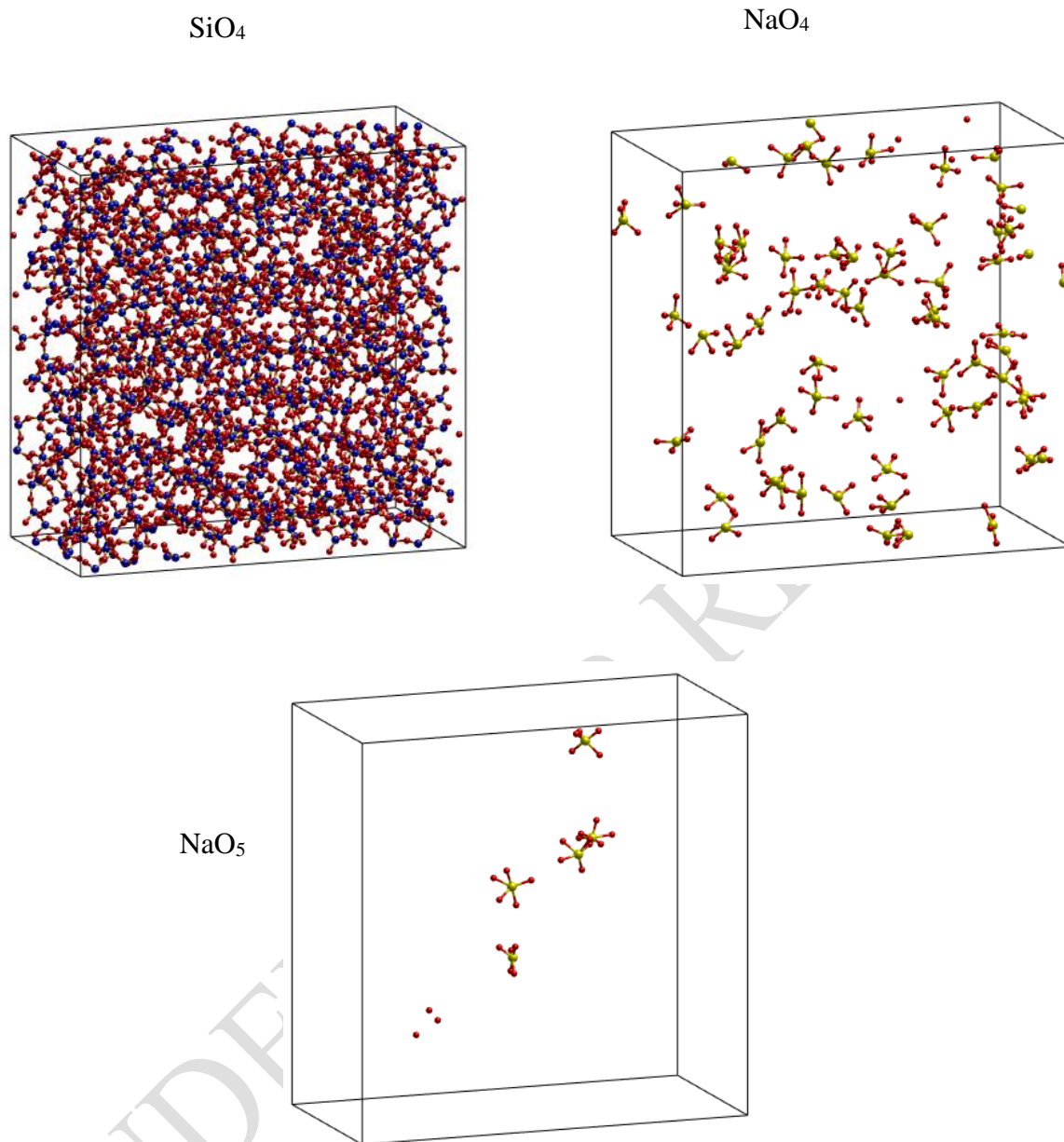


Figure 3. Spatial distribution of SiO_x and NaO_y in sample $\text{Na}_2\text{O}-3\text{SiO}_2$ at temperature of 1573 K and pressure of 0.1 MPa, here O (red color), Si (blue color), Na (yellow color).

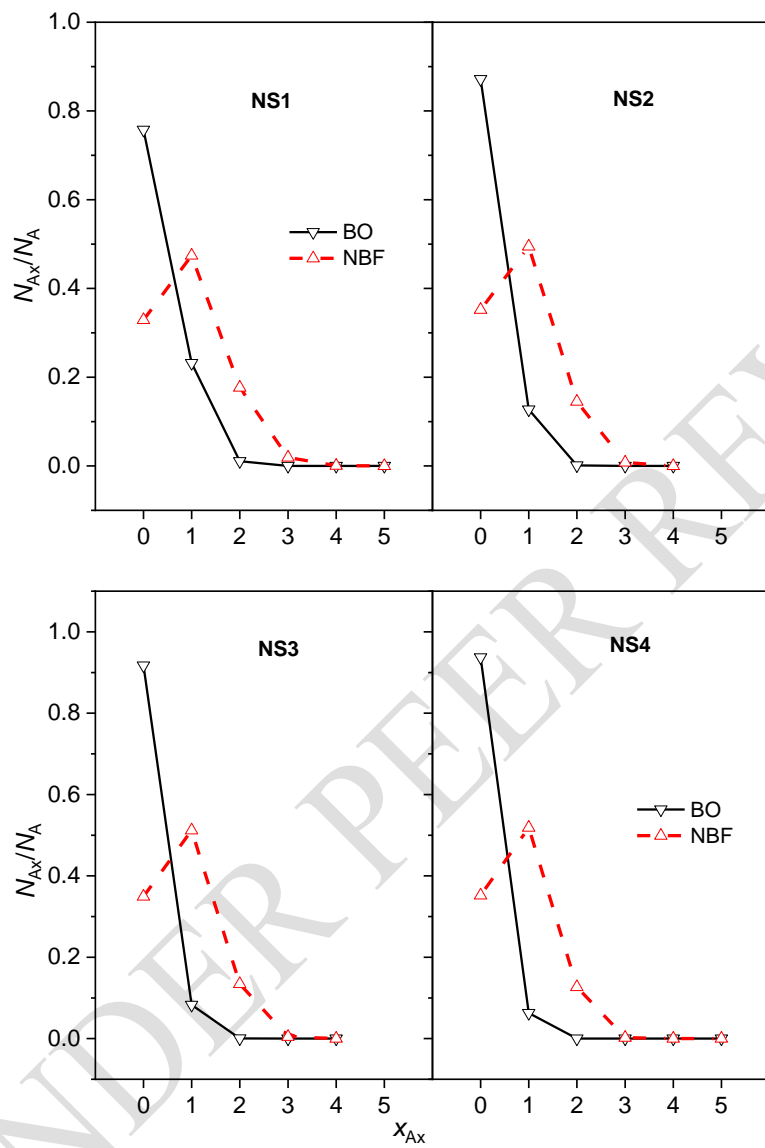


Figure 4. The fraction N_{Ax}/N_A as a function of x_{Ax} . Here N_{Ax} , N_A is the number of Ax -polyhedrons with x_{Ax} , and total number of A ; x_{Ax} is the number of N_a in Ax -polyhedron; A is the BO or NBF.

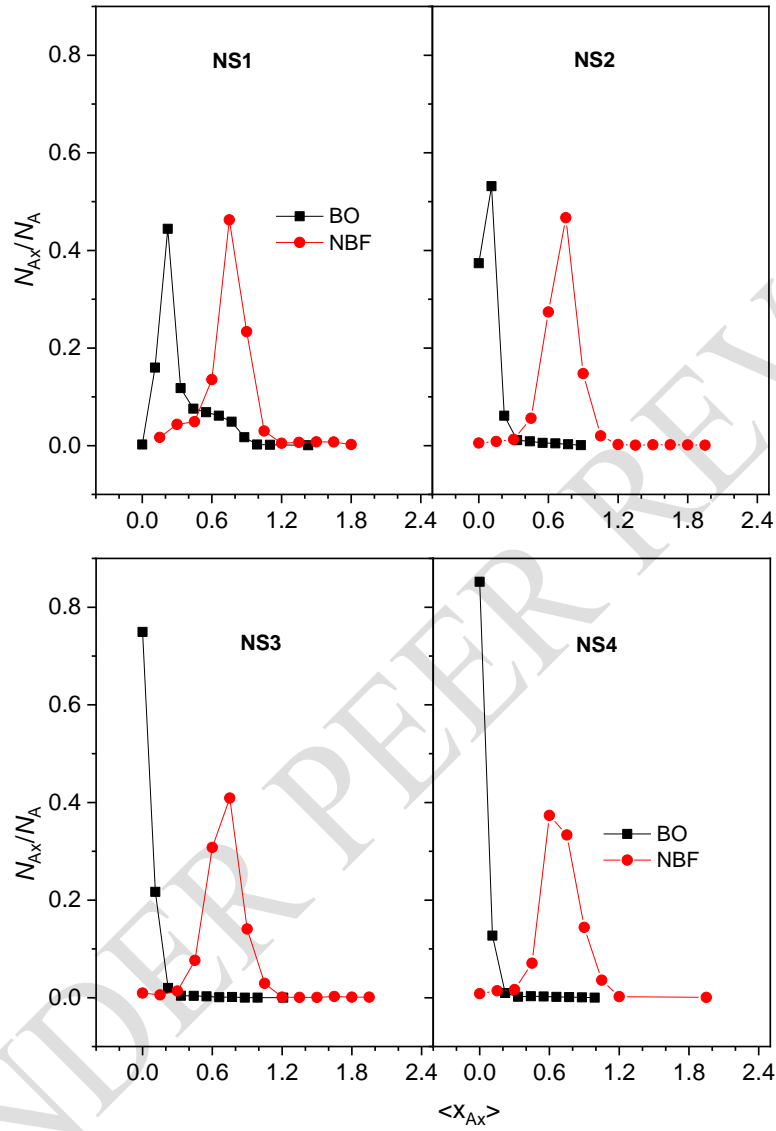


Figure 5. The fraction N_{Ax}/N_A as a function of $\langle x_{Ax} \rangle$. Here N_{Ax} , N_A is the number of Ax-polyhedrons with $\langle x_{Ax} \rangle$ and total number of BO or NBF; $\langle x_{Ax} \rangle$ is the average number of Na in Ax-polyhedron during 150 ps.